

## Structural and Electronic Properties of Novel $\pi$ -Conjugated Aniline-based Oligomers: A Computational Study

F. Kalantari Fotooh\*, M.R. Nateghi and M. Mohammadi

Department of Chemistry, Yazd Branch, Islamic Azad University, Yazd, Iran

(Received 20 February 2018, Accepted 1 June 2018)

Density functional theory (DFT) and time dependent DFT (TD-DFT) calculations were carried out for the oligomers of 3,4-Ethylenedioxythiophene-Aniline (EDOT-Ani), 3,4-Ethylenedithiafurane-Aniline (EDTF-Ani) and Thieno [3,4-b] benzene-Aniline (PITN-Ani). Structural parameters, electrical conductivity, spectral properties and electronic properties such as ionization potential (IPs), (EAs), HOMO-LUMO isosurfaces and energy gaps of EDOT-Ani, EDTF-Ani and PITN-Ani were calculated and compared using density functional theory at the B3LYP/6-31G(d) level which has been successfully used in predicting trends in conjugated systems. EDOT-Ani results showed good correlation with our previous experimental data. The vibrational frequencies with their assignments were also in close agreement with experimental frequencies. The UV-Vis spectra were simulated with TD-DFT/6-31G(d) level of theory and the maximum wavelength ( $\lambda_{\max}$ ), optical band gap ( $E_g^{\text{opt}}$ ) and oscillator strength ( $f$ ) of three oligomers were compared with each other and with experimental values. Among the studied copolymers, PITN-Ani showed the narrowest band gap which could be attributed to its higher donor acceptor property compared to two other polymers.

**Keywords:** Density functional theory, Aniline, Band gap, IR spectra, HOMO-LUMO isosurfaces

### INTRODUCTION

Electronically conducting polymers have received considerable attention because of their wide range of technological applications in optical and electronic devices [1], energy storage systems [2], solar cells [3-5], sensors [6,7] and electromagnetic shielding [8]. These applications can be attributed to their band structures. There have been a number of attempts over the past decades to present novel organic conjugated polymers with low band gaps [9,10]. It has been reported theoretically and experimentally that fusion of a benzene and thiophene in polythieno (3,4-b) benzene (PITN) increases the quinoid contribution to electronic structure and decreases the band gap [11-15]. Garcia et al. showed that the quinoid structure gives a reasonable description of PITN especially for central fragment of long oligomers [13]. Recently, PITN has been

hybridized with nano materials to improve the efficiency of dye synthesized solar cells [16,17]. Among the conjugated polymers, poly (3,4-ethylenedioxythiophen) (PEDOT) is also a promising organic electrode material because of its low band gap, low oxidation potential and remarkable environmental stability [18-22]. This polymer has chains which block the 3,4 positions of thiophene ring, exerting an electron donating effect which reduces the band gap of polythiophene to 1.2-1.7 eV and causes a high degree of visible light transmission [23,24]. Quantum chemical calculations have been employed for investigating different aspects of PEDOT [25-29]. Aleman and Casanovas have used some quantum chemical methods and investigated the conformational and electronic properties of 3,4 ethylenedioxy thiophene dimers and the material generated by interchanging the positions of oxygen and sulfur atoms [25]. Dkhissi *et al.* were applied DFT and HF methods for modeling PEDOT and PITN, and energetically show that PEDOT has an aromatic character in the ground state which

\*Corresponding author. E-mail: f-kalantari-f@iauyazd.ac.ir

is in contrast to PITN [28]. Agbaoye *et al.* calculated the elastic constants and mechanical properties of PEDOT using semi local DFT calculations [29]. Due to flexible nature of PEDOT, It can be doped with other polymers and materials to develop novel functional materials. PEDOT:PSS (poly styrene sulfonate) are being employed in electronic devices [30]. When PEDOT is doped with PSS its structure changes from benzoic shape to quinoid form [26]. Moreover, PEDOT and its derivatives with low oxidation potential and good forming ability are widely used in electrochromic materials [31-33]. A series of phenantrene centered donor-acceptor type electroactive PEDOT films with multielectrochromic properties were synthesized by Colak *et al.* [34].

In the category of conducting polymers, poly aniline has attracted much attention due to its unique doping mechanism, its ease of synthesis and high environmental and thermal stability. Several studies have been carried out for random copolymerization of aniline-EDOT monomers in order to comprise the conductivity and electro catalytic effect of both aniline and EDOT [35-38]. Copolymerization of aniline and EDOT containing nano crystalline Barium Ferrite particles show high saturation magnetization and conductivity that can be used as a microwave absorbing material [37].

In this work, using DFT-based calculations, we investigate the conformational and electronic properties of 3,4-Ethylenedioxythiophene-Aniline copolymer (n-EDOT-Ani), 3,4-ethylenedithiafurane-Ani (n-EDTF-Ani) in which the positions of the sulfur and oxygen atoms are interchanged with respect to EDOT (Fig. 1), and n-Thieno [3,4-b] benzene- Ani (n-PITN-Ani) with n ranging from 1-4. At first, we considered anti conformation for all structures and let them fully optimize. The optimized structures were used for calculating HOMO-LUMO energy gap, ionization energies, electron affinity and IR simulation. UV-Vis spectra and optical gap were also calculated using optimized structures. The obtained results are compared with available experimental data.

## COMPUTATIONAL DETAILS

In this study, three conjugated polymers with low band gap have been selected and copolymerized with aniline.

These are 3,4-Ethylenedioxythiophene-Aniline copolymer (n-EDOT-Ani), 3,4-ethylenedithiafurane-Ani (n-EDTF-Ani) and n-Thieno [3,4-b] benzene-Ani (n-PITN-Ani) with n ranging from one to four monomers. All calculations were carried out using Gaussian 09 [39] and density functional theory at the B3LYP and PBE0 methods in combination with 6-31G(d) basis set. These methods have been successfully used in predicting trends in conjugated systems without significant computational cost [40-43]. Different conformations of the dimer to tetramer forms of these copolymers were considered and the most energetically structures with lowest band gap were selected for other calculations. All structures were initially set in anti, syn, anti-syn-anti and syn-anti-conformation and were fully optimized. Ionization potentials (IPs) and electron affinities (EAs) were estimated according to the energy results of cationic and anionic forms of polymers. The HOMO-LUMO energy gap was evaluated as the difference between the highest occupied molecular orbital (HOMO) and lowest unoccupied molecular orbitals (LUMO) energy levels. IR spectra were simulated and scaled with a common scaling factor of 0.9613. Time depended DFT (TD-DFT/B3LYP/6-31G(d)) calculations were also performed for estimating the optical gap and simulation of UV-Vis spectra in DMSO medium on polarized continuum model (PCM).

## RESULTS AND DISCUSSION

### Structural Parameters

Three copolymers were initially set in four conformers (Fig. 1) and fully optimized. The most energetically stable structures were selected for other calculations. Optimized structures of 4-EDOT-Ani, 4-EDTF-Ani and 4-PITN-Ani structures are presented in Fig. 2. It can be seen that after full optimization, bridging angles change and all geometries are in twisted manner to minimize steric hindrance of cycles. The torsional angles between cycles are presented in Table 1.

Structural results of EDOT-Ani show a syn-gauche conformation after full relaxation. The torsional angle between EDOT and aniline which are bonded with C-C bond, is about 20-23°. Anyway, the torsional angle between two monomers at C-N bond is about 58-60°. The interring distance is 1.46 Å for C-C and about 1.39-1.40 Å for N-C

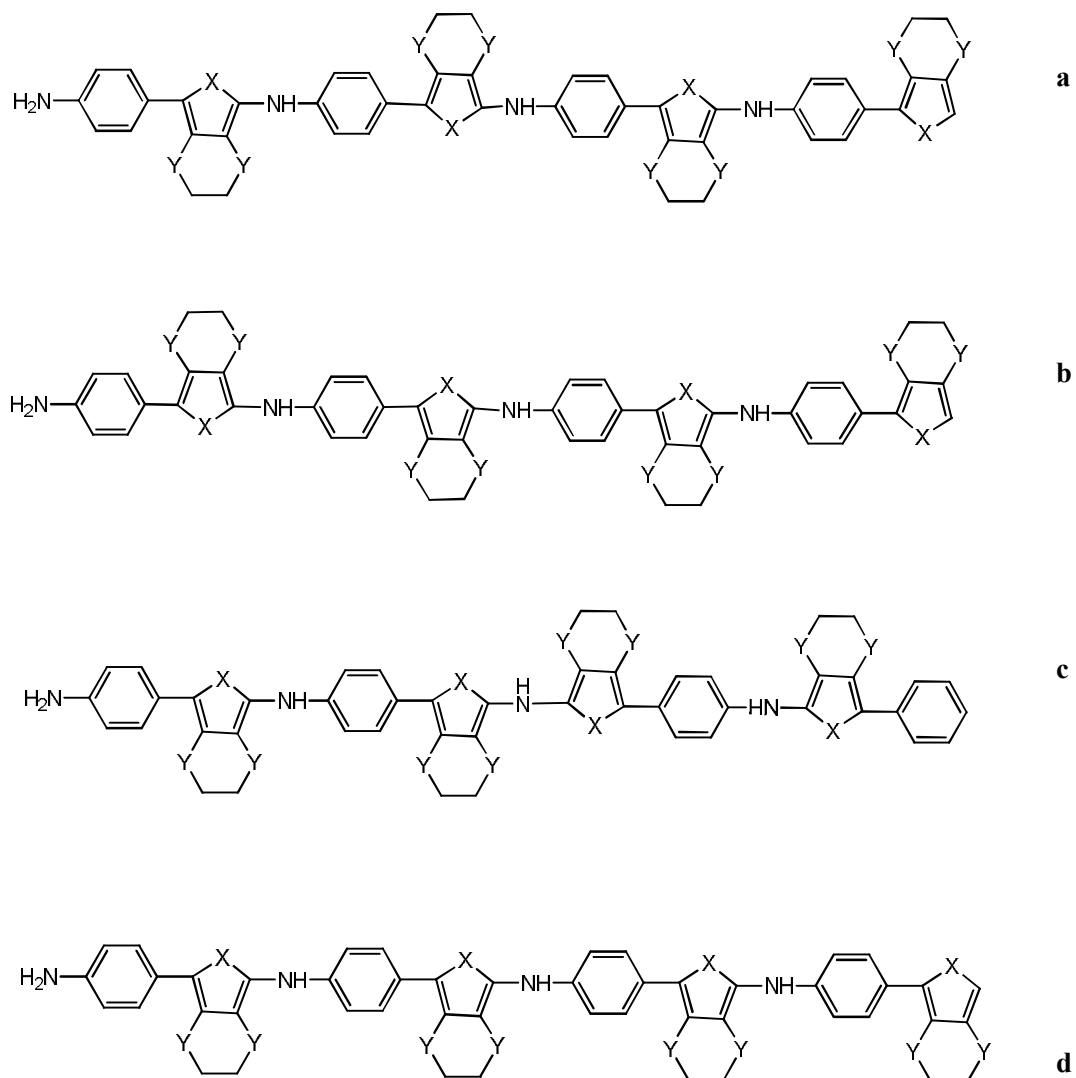


**Fig. 1.** a) Anti, b) anti-syn-anti, c) syn-anti-syn and d) syn conformations of the studied co-polymers.

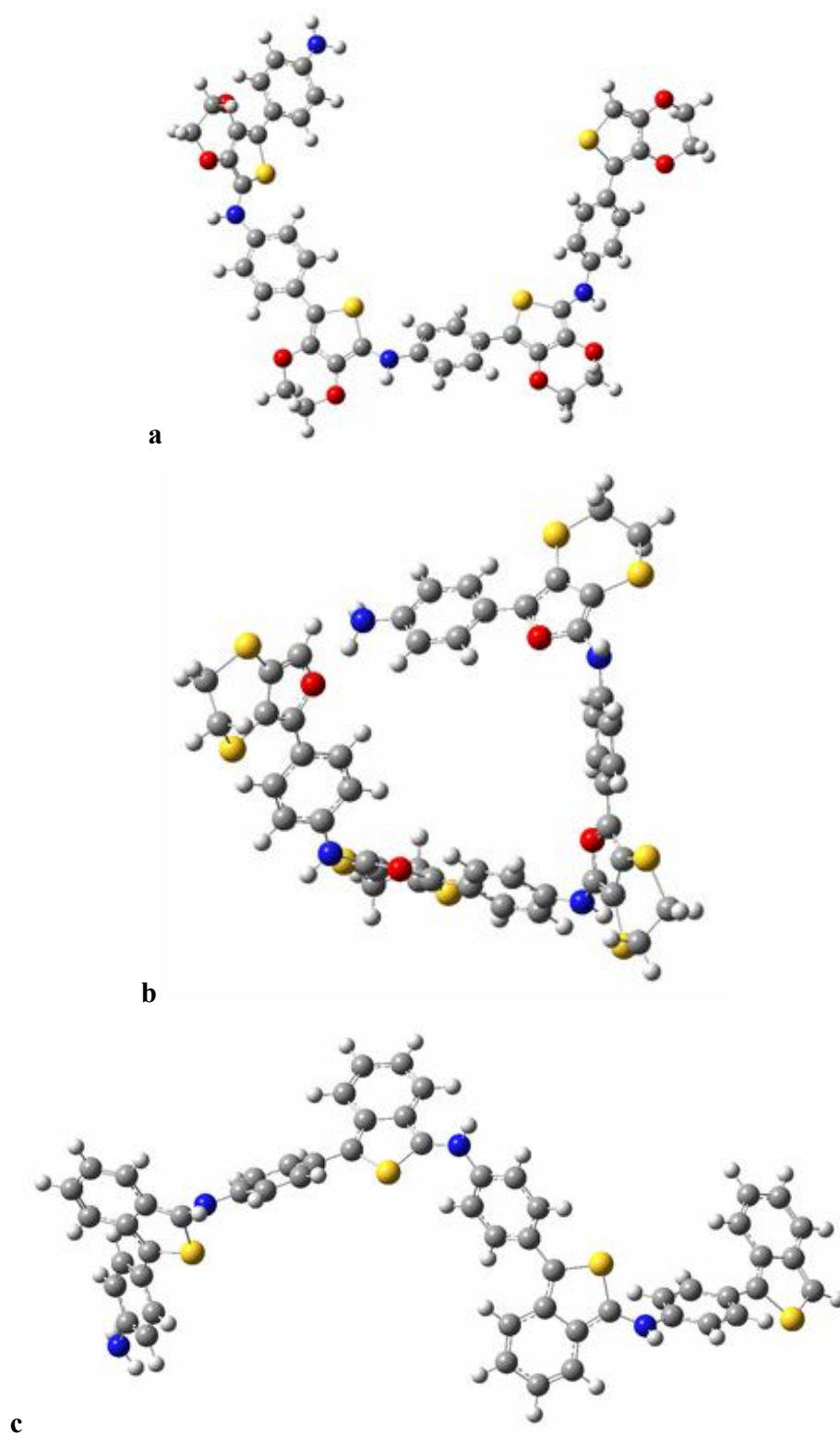
bond lengths indicating the benzoid structure of these copolymers [44]. EDTF-Ani structure is twisted more than EDOT-Ani. The torsional angles at C-C interring bond change from 14-25° and the torsional angles between two monomers at C-N bond are varying between 50-60°. The monomers are in syn-gauche conformation after full optimization.

The inter ring distances are the same as EDOT-Ani distances. After full geometry optimization in PITN-Ani, the structure changes considerably and achieves zigzag geometry. Bond length extensions are slightly higher than

those in EDTF-Ani and EDOT-Ani copolymers. They are 1.40 Å for N-C and 1.47 Å for C-C bonds. Inter ring torsional angles are more extended than two other structures. They are about 40-41° at C-C bond and about 130° between two monomers at C-N bond. Higher inter ring torsional angles and longer inter ring bond lengths show its lower conjugation compared with previous co-polymers.

### Electronic Properties

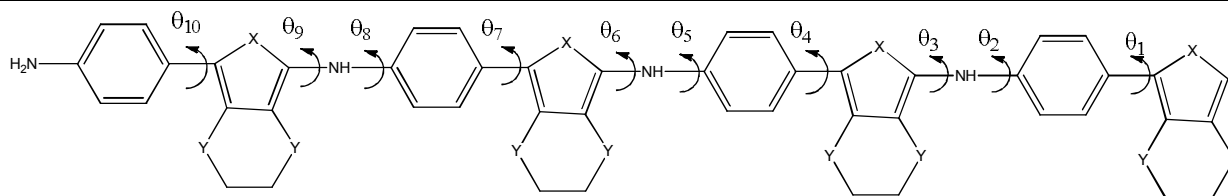
In this section, we investigate the HOMO/LUMO energies, energy gaps of copolymers, and the effect of



**Fig. 2.** Optimized structure of a) 4-EDOT-Ani, b) 4-EDTF-Ani and c) 4-PITN-Ani using B3LYP/6-31G\* method.

**Table 1.** Torsional Angles (in Degree) of the Studied Structures after Full Optimization Using B3LYP/6-31G\*. The Angles are Shown in the Figure Below. X = S and Y = O for EDOT-Ani, X = O and Y = S for EDTF and X = S and Y = (C=) for PITN-Ani

	$\theta_1$	$\theta_2$	$\theta_3$	$\theta_4$	$\theta_5$	$\theta_6$	$\theta_7$	$\theta_8$	$\theta_9$	$\theta_{10}$
EDOT-Ani	-22.4	3.782	58.41	23.18	-0.39	-57.63	19.46	-0.34	59.20	-20.8
EDTF-Ani	24.9	8.148	60.08	-16.93	-17.8	-49.8	-15.40	20.97	54.82	14.27
PITN-Ani	41.79	-20.19	129.7	-39.86	19.60	-130.4	39.5	18.7	-128.4	39.8

**Table 2.** HOMO-LUMO Energies (in eV) and Energy Gaps (EH-L) Calculated Using B3LYP/6-31G\* and PBE0/6-31G\* for Monomer to Tetramer Forms of EDOT-Ani, EDTF-Ani and PITN-Ani

Structure	B3LYP			PBE0			
	HOMO/eV	LUMO/eV	E <sup>H-L</sup>	HOMO/eV	LUMO/eV	E <sup>H-L</sup>	
EDOT-Ani	Monomer	-4.83	-0.503	4.32	-5.06	-0.36	4.70
	Dimer	-4.38	-0.718	3.66	-4.61	-0.587	4.02
	Trimer	-4.31	-0.777	3.53	-4.89	-0.569	4.32
	Tetramer	-4.19	-0.812	3.37	-4.54	-0.686	3.85
EDTF-Ani	Monomer	-4.82	-0.419	4.40	-5.03	-0.28	4.75
	Dimer	-4.46	-0.650	3.81	-4.64	-0.551	4.09
	Trimer	-4.38	-0.686	3.69	-4.57	-0.587	3.98
	Tetramer	-4.52	-0.730	3.78	-4.7	-0.577	4.12
PITN-Ani	Monomer	-4.81	-1.30	3.51	-5.05	-1.19	3.87
	Dimer	-4.77	-1.51	3.26	-5.03	-1.41	3.62
	Trimer	-4.73	-1.59	3.14	-4.99	-1.46	3.53
	Tetramer	-4.59	-1.63	2.96	-4.91	-1.49	3.42

structure on energy levels and conductivity. The HOMO/LUMO energy levels for monomer to tetramer forms of the studied co-oligomers are presented in Table 2. The results indicate that by increasing the number of monomers, the energies of LUMO states reduce and the energies of HOMO states increase in all structures, which help the coupling between the neighboring units. Higher planarity of EDOT-Ani compared to EDTF-Ani helps the increasing of the HOMO energies and stabilizing the LUMOs. So, the conjugation along the chain increases and the band gap reduces. In three studied oligomers, the gap decreases when  $n$  increases. The H-L gap ( $E^{H-L}$ ) is obtained about 3.37 eV for 4-EDOT-Ani and 3.78 eV for 4-EDTF-Ani. The energy gaps of dimer structures are lower than those obtained computationally for 2-EDOT (4.06 eV) and 2-EDTF (3.99 eV) [25]. So, Aniline part of these co-oligomers reduces the energy gaps and increases the conductivity of the polymer. PITN-Ani has the lowest energy gap among the studied molecules. This is while it was shown that PITN-Ani has the lowest planarity. Therefore, its lower energy gap compared with EDOT-Ani and EDTF-Ani can be attributed to its higher donor-acceptor interactions along the polymer chain [44].

To compare different DFT functionals, PBE0 energy gaps are also presented in Table 2. PBE0 functional was proposed to be reliable for predicting the band gaps of conjugated polymers [42]. The energy results show that PBE0 gives higher energies than B3LYP as predicted previously [42]. Band gaps obtained using PBE0 are higher than those calculated using B3LYP functional. This is due to more stabilization of the HOMO states and destabilization of LUMO states at PBE0/6-31G (d) level. The adiabatic electron affinity (EA) and ionization potential (IP) are defined as:

$$EA = E_{\text{neutral}} - E_{\text{anion}} \quad (1)$$

$$IP = E_{\text{cation}} - E_{\text{neutral}} \quad (2)$$

where  $E_{\text{neutral}}$  is the total energy of neutral molecule at its optimized geometry.  $E_{\text{anion}}$  and  $E_{\text{cation}}$  are the total energies of corresponding anion and cation calculated at their optimized geometry.

The results presented in Table 3 show a little difference

between IPs of three families of heterocyclic compounds. By increasing the energies of HOMO state, the IP reduces. Among the studied copolymers, PITN-Ani has the highest IPs. Therefore EDOT-Ani and EDTF-Ani co-oligomers tend to be oxidized more easily than PITN-Ani oligomer. By increasing the number of monomers, the energies of HOMO states increase and the LUMO states are stabilized, so, the IP and the EA in all three co-oligomers reduce and increase, respectively. The results show that EA values of EDOT-Ani and EDTF-Ani are negative while the EA values of 2-4-PITN-Ani are positive. The negative EA value show that the conduction band edge is above the vacuum level and the positive values of PITN show that the conduction band edge is below the vacuum level. As can be seen from Table 3, LUMO of PITN is lower and can be reduced better than EDOT-Ani and EDTF-Ani co-oligomers. The IPs obtained using PBE0 functional are close to those of B3LYP. By increasing the number of monomers, PBE0 functional overestimates the EA of oligomers. However, two computational methods show the same trend for EA, IP and HOMO-LUMO energies.

Isosurfaces plots of HOMO and LUMO are depicted in Figs. 3-5. In All three monomers, the HOMO and LUMO orbitals are extended throughout the optimized structures. The HOMO is mostly concentrated on aromatic rings and the LUMO is located on inter ring C-C bond, indicating the benzoid character of these monomers. However, in 1-PITN-Ani HOMO spreads over the entire frame of molecule and the C-C interring bond, confirming the electron conjugation between PITN and Aniline ring. By increasing the number of monomers,  $\pi$  orbitals are delocalized over the entire frame of oligomers, so, the electron density of HOMO and LUMO decreases. This delocalization increases the conjugation and subsequently enhances the conductivity.

Another factor affecting on delocalization is the torsional angles. By increasing the non-planarity of conjugated backbone, the delocalization reduces [9]. As can be seen from the figures, in tetramer structures, the HOMOs are mostly prominent over the N atom of aniline and C atom of adjacent monomer. This indicates the effect of N atom of aniline on conjugation. It can be seen from Fig. 5 that LUMO states of PITN-Ani are mostly localized over PITN. This result can be attributed to acceptor moiety of PITN.

**Table 3.** Adiabatic Electron Affinity (EA), and Ionization Potentials (IP) Calculated Using B3LYP/6-31G\* and PBE0/6-31G\* Methods for Monomer to Tetramer Forms of EDOT-Ani, EDTF-Ani and PITN-Ani

	Structure	B3LYP		PBE0	
		IP (eV)	EA (eV)	IP (eV)	EA (eV)
EDOT-Ani	Monomer	6.440	-1.10	6.527	-1.10
	Dimer	5.563	-0.431	5.688	-0.462
	Trimer	5.282	-0.167	5.778	-0.361
	Tetramer	5.043	-0.023	5.352	-0.125
EDTF-Ani	Monomer	6.363	-1.146	6.441	-1.133
	Dimer	5.606	-0.484	5.686	-0.482
	Trimer	5.378	-0.259	5.473	-0.283
	Tetramer	5.341	-0.108	5.486	-0.205
PITN-Ani	Monomer	6.338	-0.289	6.439	-0.265
	Dimer	5.904	0.329	6.084	0.3063
	Trimer	5.617	0.623	5.848	0.5611
	Tetramer	5.388	0.822	5.672	0.7388

### UV-Vis Spectra

The theoretically simulated UV-Vis spectra of EDOT-Ani, EDTF-Ani and PITN-Ani oligomers at the TD-DFT/6-31G\* level of theory are given in Fig. 6 for all conformations. The UV-Vis spectrum of EDOT consists mainly of five distinctive absorptions at 424, 380, 367, 346 and 305 nm. The peaks at 300-367 nm correspond to  $\pi$ - $\pi^*$  excitation of the *para* substituted benzene segment in Aniline. The broad peak at 420- 426 nm can be attributed to  $\pi$ - $\pi^*$  electronic transition of EDOT ring. Two peaks at 446 and 424 nm are in agreement with experimental results [38] at 410 and 330 nm. The difference between experimental and theoretical results is due to the gas phase and oligomer study in our work.

By S/O substituting in EDTF-Ani, a hypsochromic shift is observed which is due to greater steric factor and its

lower conjugation compared to EDOT-Ani. The broad peak at about 380 nm is attributed to  $\pi$ - $\pi^*$  electronic transition of EDTF ring, and a peak around 310 nm corresponds to  $\pi$ - $\pi^*$  excitation of the *para* substituted benzene segment in aniline.

A bathochromic effect with lesser extent is observed for 4- PITN-Ani compared with 4-EDOT-Ani and 4-EDTF-Ani oligomers, indicating the delocalization in aromatic ring of this oligomer. It seems that an acceptor property of PITN shifts the aniline peak to higher wavelength. Maximum wavelength ( $\lambda_{\max}$ ), optical band gap ( $E_g^{\text{opt}}$ ) and oscillator strength ( $f$ ), calculated using TDDFT/B3LYP/6-31G\* method, are presented in Table 4. The results show the highest  $\lambda_{\max}$  for PITN-Ani and the lowest one for EDTF-Ani copolymer. The computed values of  $E_g^{\text{opt}}$  represent the vertical excitation energies from the ground state to the first



**Fig. 3.** Isosurfaces plots of HOMO and LUMO states of 1,4 EDOT-Ani from B3LYP/6-31G\* level with isodensity value = 0.02 *au*. The electron accumulation is indicated with yellow and the charge depletion with red colors.

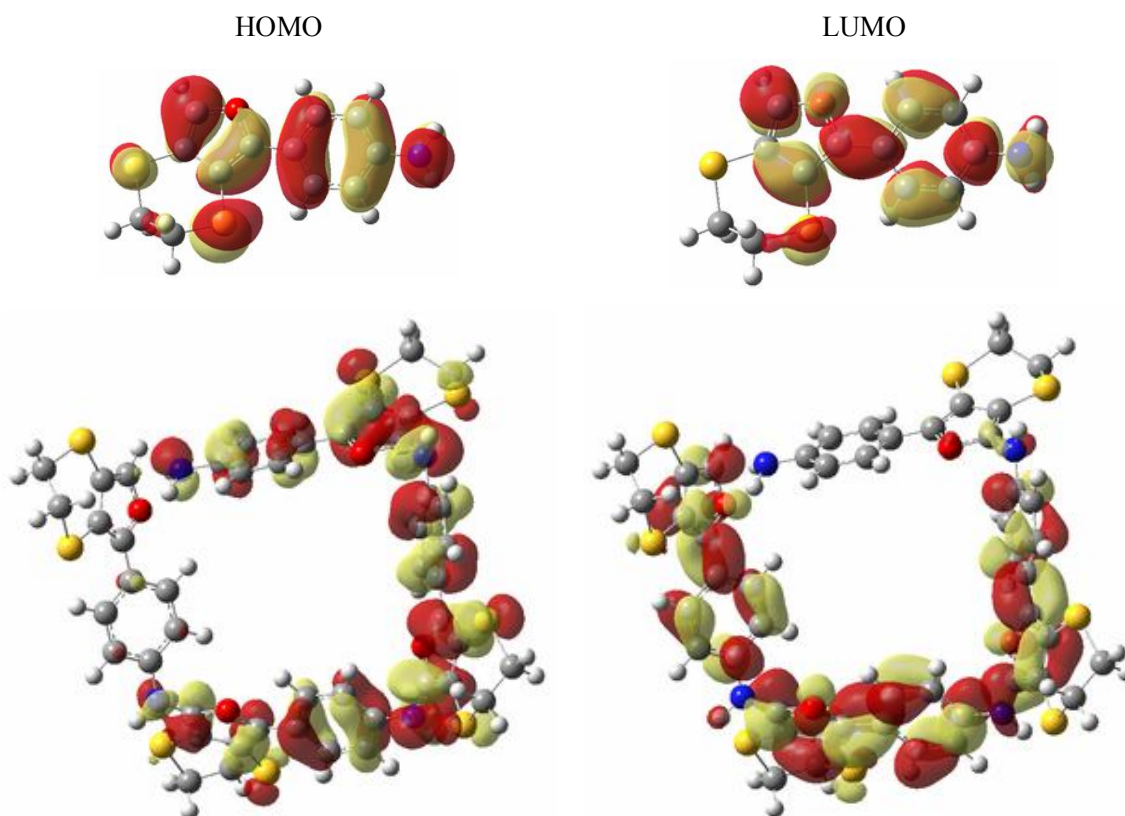


**Fig. 4.** Isosurfaces plots of HOMO and LUMO states of 1,4 EDTF-Ani at the B3LYP/6-31G\* level with isodensity value = 0.02 *au*. The electron accumulation is indicated with yellow and the charge depletion with red colors.

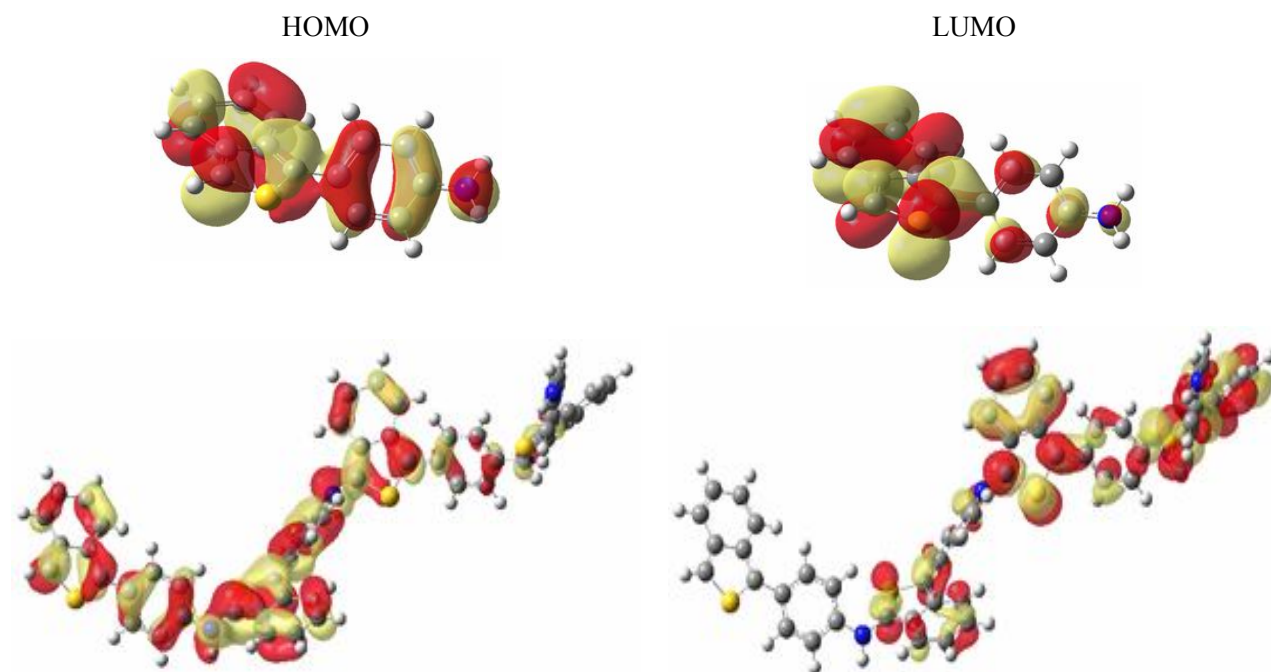


**Fig. 5.** Isosurfaces plots of HOMO and LUMO states of 1,4 PITN-Ani at the B3LYP/6-31G\* level with isodensity value = 0.02 *au*. The electron accumulation is indicated with yellow and the charge depletion with red colors.

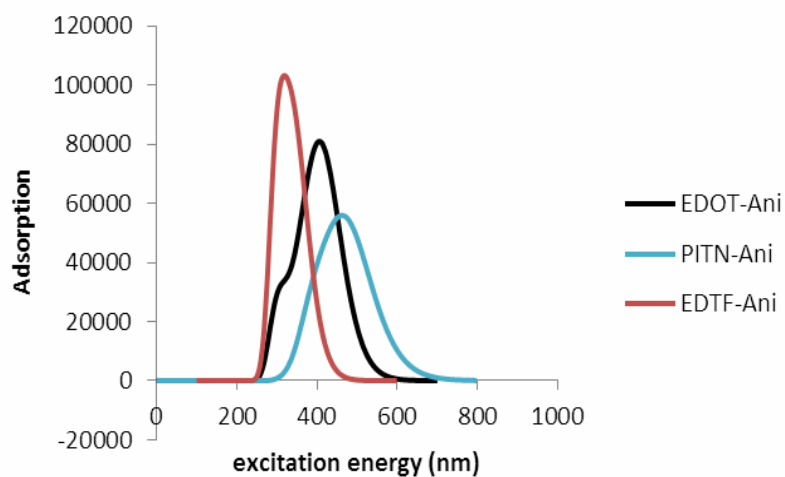


**Fig. 6.** UV-Vis. spectra of three studied copolymers at the TDDFT/B3LYP/6-31G\* level.

excited state and are directly comparable to the optical band gap observed from UV-Vis absorption spectroscopy [45-48]. The computed values of  $E_g^{H-L}$  represent the valence to conduction band energy difference in the ground state and

are directly comparable to the band gap measured from cyclic voltammetry.

The results show that the optical band gap of EDOT-Ani is about 2.92 eV in close agreement with experimental value

**Table 4.** Maximum Wavelength ( $\lambda_{\max}$ ) in nm, Optical Band Gap ( $E_g^{\text{opt}}$ ) in eV, Oscillator Straight (f) and Exciton Binding Energy ( $E_B$ ) in eV, Calculated Using TDDFT/B3LYP/6-31G\* and TDDFT/PBE0/6-31G\* Methods

		$E_g^{\text{opt}}$	$\lambda_{\max}$	f	$E_B$
B3LYP	4-EDOT-Ani	2.92	424.46	1.4435	0.4538
	4-EDTF-Ani	3.27	379.69	0.2497	0.5194
	4-PITN-Ani	2.53	490.28	0.8393	0.4325
PBE0	4-EDOT-Ani	3.16	392.21	1.118	0.6900
	4-EDTF-Ani	3.68	337.22	0.71	0.4478
	4-PITN-Ani	2.79	443.89	0.8428	0.6233

(2.88 eV) [38]. The highest optical band gap belongs to EDTF-Ani oligomer with lower conjugation. The results show that  $E_g^{\text{H-L}}$  values are all greater than  $E_g^{\text{opt}}$  values since they take additional energies to fully separate the electrons and holes into free carriers [49]. The difference in  $E_g^{\text{H-L}}$  and  $E_g^{\text{opt}}$  is called the exciton binding energy ( $E_B$ ) which is higher for EDTF-Ani oligomer. TDDFT results obtained using PBE0 functional are also presented in Table 4 for comparison. The results show that PBE0 calculations overestimate the optical band gap with higher discrepancy from experimental data. The maximum wavelengths are lower than those in B3LYP results.

### IR Studies of Oligomers

The theoretically simulated IR spectrum of 4-EDOT-Ani copolymer is presented in Fig. 7. These spectra are calculated by B3LYP/6-31G\* method and systematic errors in calculations are removed by applying a scaling factor of 0.9613 [39,50].

The major peaks values of three conjugated oligomers along with available experimental bands are given in Table 5. A peak at about 3446-3505  $\text{cm}^{-1}$  is assigned to N-H stretching. The difference in simulated and observed N-H stretching can be attributed to the fact that theoretical data is for an isolated oligomer in vacuum state while the experimental is that of condensed phase. The bands at 2930 and 3066  $\text{cm}^{-1}$  are assignable to asymmetric C-H stretching

of dioxan and aniline rings, respectively. The band around 1582- 1606  $\text{cm}^{-1}$  are corresponding to C-C and C=C stretching of thiophen ring. It was theoretically predicted that in PEDOT, C-C and C=C bands are appeared about 1454  $\text{cm}^{-1}$  and 1370  $\text{cm}^{-1}$ . So, aniline ring shifts PEDOT frequencies to higher values [28]. The vibration at 1077  $\text{cm}^{-1}$  is assigned to C-O-C bond stretching in the ethylenedioxy group. C-S stretching band is observed at about 814  $\text{cm}^{-1}$ . These results are in close agreement with experimental data [38].

By replacing the thiophen ring with furan the C=C frequency of aniline ring shifts slightly to higher frequencies. The band at 2951-3004  $\text{cm}^{-1}$  can be attributed to C-H stretching of dithiophen ring. A peak at 1030  $\text{cm}^{-1}$  is assigned to C-O of furan ring. The vibrations at 961-978  $\text{cm}^{-1}$  are assignable to C-S bond stretching in dithiophen ring. In PITN, N-H stretching peak shifts to lower frequency and appears at 3416  $\text{cm}^{-1}$ . The bands at 1600, 1515 and 1414  $\text{cm}^{-1}$  are corresponding to aniline, thiophen and benzene rings, respectively. The vibrations at 849  $\text{cm}^{-1}$  are assignable to C-S bond stretching in thiophen ring. N-H bending is appeared at 350  $\text{cm}^{-1}$ .

### CONCLUSIONS

DFT quantum mechanical calculations have been performed to examine and compare the structural parameter,

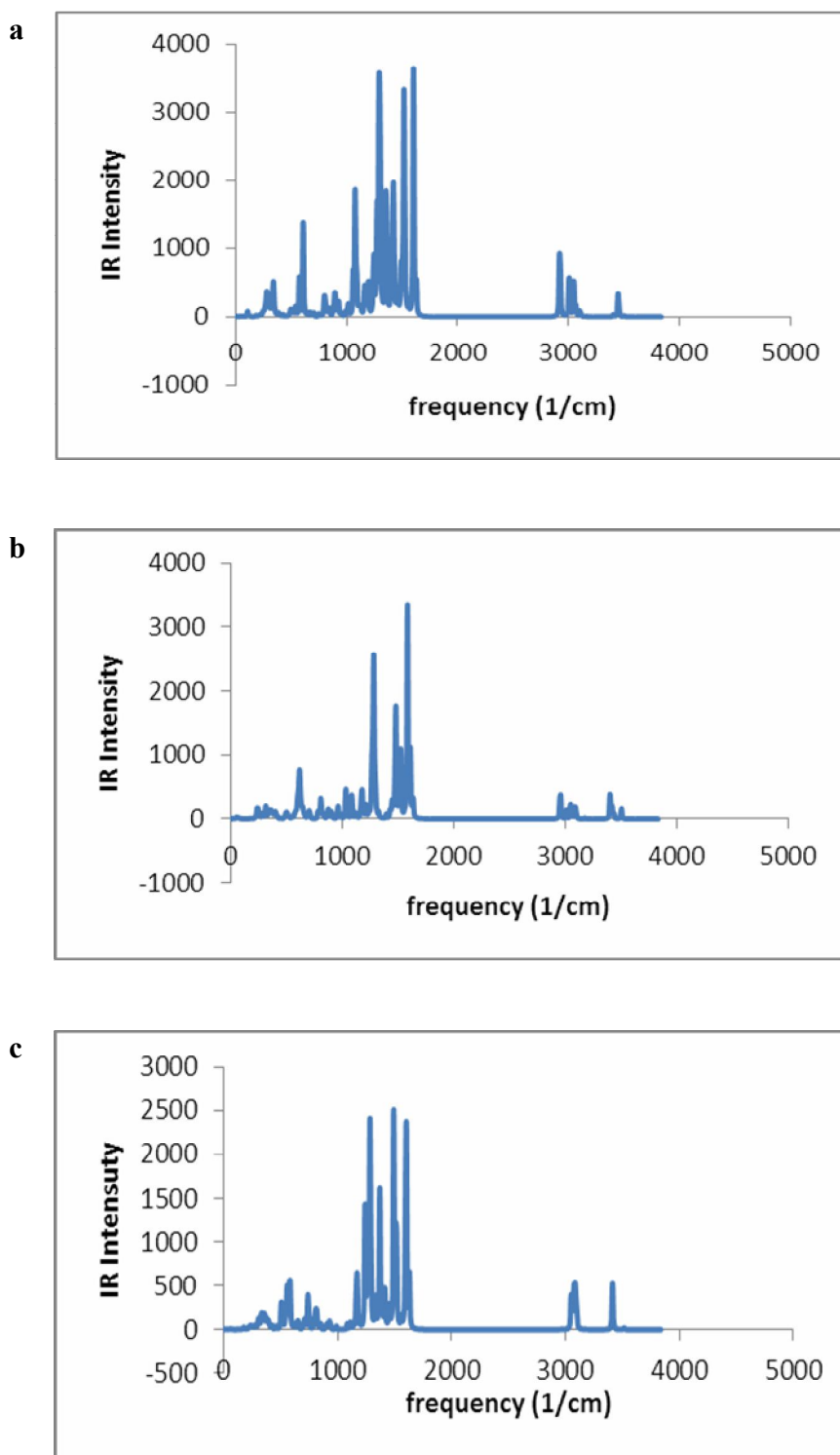


Fig. 7. Scaled IR spectra of a) 4-EDOT-Ani b) 4-EDTF-Ani and c) 4-PITN- Ani oligomers.

**Table 5.** Calculated IR Frequencies ( $\text{cm}^{-1}$ ) of EDOT-Ani, EDTF-Ani and PITN-Ani co-oligomers

EDOT-Ani			EDTF-Ani		PITN-Ani	
Calculated frequency	experimental I.R [38]	Approximated assignment	Calculated frequency	Approximated assignment	Calculated frequency	Approximated assignment
3446-3503	3345	v-NH	3420-3504	v-NH	3416	v-NH
2930-3011		v-CH <sub>2</sub> (dioxan)	2951-3004	v-CH <sub>2</sub> (dioxan)	3078-3093	v-CH (aromatic)
2930-3066		v-CH (aniline)	3051-3088	v-CH (aniline)	1600	v-C=C(ani)
1582-1604		v-C=C, thiophen	1544	v-C=C, furan	1515	v-C=C(thio)
1606		v-C=C(ani)	1610	v-C=C(ani)	1389-1414	v-C-C,C-
1563-1559	1621	$\beta$ -N-H, v-C=C(ani)	1564-1566	$\beta$ -N-H, v-C=C(ani)		N(interring), C=C
1521	1487-1621	v-C-C,C-N(interring), C=C	1510-1528	v-C-C,C-N(interring), C=C	1371	rockingC-H (aniline), N-H
1356	1360	wag CH <sub>2</sub> (dioxan)	1296	wag CH <sub>2</sub> (dioxan)	1283	v-C=C,C-N
1294-1304		rockingC-H (aniline)	1298	rockingC-H (aniline)	849.3	v C-S
1077	1081	v C-O	1030	v C-O	567	Ring (Def)
814.2	826	v C-S	961-978	v C-S	350.2	$\beta$ -N-H
802.7		v C-H wag	807			
613.3		Def(r), wagN-H	617-605	Def(r), wagN-H		

spectral properties and electronic properties such as HOMO, LUMO, IP, EA and energy gap. The optimized geometries are found to be in twisted and zigzag. The optimized bond lengths and angles show the benzoid structure of these copolymers. The electronic results show that

copolymerization of the studied compounds with aniline increases their conductivity. PITN-Ani has the highest IP and the lowest EA among the studied polymers. So, this copolymer is reduced better than EDOT-Ani and EDTF-Ani. The results show the narrowest band gap for PITN-

Ani, due to higher acceptor property of PITN compared to EDOT or EDTF. Isosurfaces plots of HOMO and LUMO show that in tetramer structures, the HOMO is more prominent over the N-C inter ring bonds, due to nitrogen conjugation with thiophen or furan rings. The  $\pi$ - $\pi^*$  transition of UV-Vis spectrum of EDOT-Ani, EDTF-Ani and PITN-Ani together with optical gap and  $\lambda_{\text{max}}$  are calculated using TD-DFT/6-31G\* method. The results show good correlation with EDOT-Ani experimental values. PITN-Ani shows the lowest energy gap and the highest wavelength. This bathochromic effect shows the delocalization in aromatic ring of this copolymer. The quoted values of I.R spectrum evaluated at the same level of theory are in good agreement with experimental data.

## REFERENCES

- [1] He, H.; Zhu, J.; Tao, N. J.; Nagahara, L. A.; Amlani, I.; Tsui, R., A conducting polymer nanojunction switch. *J. Am. Chem. Soc.*, **2001**, *123*, 7730-7731, DOI: 10.1021/ja016264i.
- [2] Cheng, F.; Tang, W.; Li, C.; Chen, J.; Liu, H.; Shen, P.; Dou, S., Conducting poly(aniline) nanotubes and nanofibers: Controlled synthesis and application in lithium/poly(aniline) rechargeable batteries. *Chem. Eur. J.*, **2006**, *12*, 3082-3088, DOI: 10.1002/chem.200500883.
- [3] Krebs, F. C., Fabrication and processing of polymer solar cells: A review of printing and coating techniques. *Solar Energy Mater. Solar Cells* **2009**, *93*, 394-412, DOI: <https://doi.org/10.1016/j.solmat.2008.10.004>.
- [4] Yue, D.; Khatav, P.; You, F.; Darling, S. B., Deciphering the uncertainties in life cycle energy and environmental analysis of organic photovoltaics. *Energy & Environ. Sci.* **2012**, *5*, 9163-9172, DOI: 10.1039/C2EE22597B.
- [5] Xu, T.; Yu, L., How to design low bandgap polymers for highly efficient organic solar cells. *Mater. Today* **2014**, *17*, 11-15, DOI: <https://doi.org/10.1016/j.mattod.2013.12.005>.
- [6] Li, L.; Wang, Y.; Pan, L.; Shi, Y.; Cheng, W.; Shi, Y.; Yu, G., A nanostructured conductive hydrogels-based biosensor platform for human Metabolite Detection. *Nano Lett.* **2015**, *15*, 1146-1151, DOI: 10.1021/nl504217p.
- [7] Dunst, K.; Karczewski, J.; Jasiński, P., Nitrogen dioxide sensing properties of PEDOT polymer films. *Sensors and Actuators B: Chem.* **2017**, *247*, 108-113, DOI: <http://dx.doi.org/10.1016/j.snb.2017.03.003>.
- [8] Ullah, H.; Shah, A.-u.-H. A.; Ayub, K.; Bilal, S., Density functional theory study of poly(o-phenylenediamine) oligomers. *J. Phys. Chem. C* **2013**, *117*, 4069-4078, DOI: 10.1021/jp311526u.
- [9] Bhatta, R. S.; Tsige, M., Understanding the effect of heteroatoms on structural and electronic properties of conjugated polymers. *Polymer* **2015**, *56*, 293-299, DOI: <http://dx.doi.org/10.1016/j.polymer.2014.11.050>.
- [10] Govindaraju, K. M.; Prakash, V. C. A., Synthesis of zinc modified poly(aniline-co-pyrrole) coatings and its anti-corrosive performance on low nickel stainless steel. *Colloids and Surfaces A: Physicochem. Engin. Aspects* **2015**, *465*, 11-19, DOI: <https://doi.org/10.1016/j.colsurfa.2014.10.011>.
- [11] Brocks, G., Density functional study of polythiophene derivatives. *J. Phys. Chem.* **1996**, *100*, 17327-17333, DOI: 10.1021/jp962106f.
- [12] Paulussen, H.; Ottenbourgs, B.; Vanderzande, D.; Adriaensens, P.; Gelan, J., Synthesis of poly(isothianaphthene) from 1,1,3,3-tetrachlorothio-phthalan and tert-butylmercaptan: mechanism and quantitative analysis by solid state n.m.r. *Polymer* **1997**, *38*, 5221-5225, DOI: [http://dx.doi.org/10.1016/S0032-3861\(97\)00036-0](http://dx.doi.org/10.1016/S0032-3861(97)00036-0).
- [13] Garcia, M.; Ramos, E.; Guadarrama, P.; Fomine, S., Electronic structures of neutral, cationic and dicationic states of the low band gap polymers. Polythieno[3,4-b]benzene, a case study. *Synth. Met* **2009**, *159*, 2081-2085, DOI: <http://dx.doi.org/10.1016/j.synthmet.2009.07.030>.
- [14] Borrelli, D. C.; Gleason, K. K., Tunable low bandgap polyisothianaphthene via oxidative chemical vapor deposition. *Macromolecules* **2013**, *46*, 6169-6176, DOI: 10.1021/ma400890a.
- [15] Chen, W. -T.; Bowmaker, G. A.; Seakins, J. M.; Cooney, R. P., Modified synthetic routes to

- poly(isothianaphthene). *Synth. Met.* **2002**, *128*, 215-220, DOI: [http://dx.doi.org/10.1016/S0379-6779\(02\)00022-X](http://dx.doi.org/10.1016/S0379-6779(02)00022-X).
- [16] Ramar, A.; Saraswathi, R.; Rajkumar, M.; Chen, S.-M., TiO<sub>2</sub>/polyisothianaphthene-A novel hybrid nanocomposite as highly efficient photoanode in dye sensitized solar cell. *J. Photochem. Photobiol. A: Chem.*, **2016**, *329*, 96-104, DOI: <http://dx.doi.org/10.1016/j.jphotochem.2016.05.028>.
- [17] Ramar, A.; Saraswathi, R.; Vilian, A. T. E.; Chen, S.-M.; Wang, F. -M., Polyisothianaphthene/graphene nanocomposite as a new counter electrode material for high performance dye sensitized solar cell. *Synth. Met.* **2017**, *230*, 58-64, DOI: <http://dx.doi.org/10.1016/j.synthmet.2017.05.016>.
- [18] Groenendaal, L.; Jonas, F.; Freitag, D.; Pielartzik, H.; Reynolds, J. R., Poly(3,4-ethylenedioxythiophene) and its derivatives: Past, present, and future. *Adv. Mater.* **2000**, *12*, 481-494, DOI: 10.1002/(SICI)1521-4095(200004)12:7<481::AID-ADMA481>3.0.CO;2-C.
- [19] Apperloo, J. J.; Groenendaal, L. B.; Verheyen, H.; Jayakannan, M.; Janssen, R. A. J.; Dkhissi, A.; Beljonne, D.; Lazzaroni, R.; Brédas, J. -L., Optical and redox properties of a series of 3,4-ethylenedioxythiophene oligomers. *Chem. Eur. J.* **2002**, *8*, 2384-2396, DOI: 10.1002/1521-3765(20020517)8:10<2384::AID-CHEM2384>3.0.CO;2-L.
- [20] Yu, J.; Holdcroft, S., Synthesis, solid-phase reaction, and patterning of acid-labile 3,4-ethylenedioxythiophene-based conjugated polymers. *Chem. Mater.* **2002**, *14*, 3705-3714, DOI: 10.1021/cm020113c.
- [21] Najeeb, M. A.; Abdullah, S. M.; Aziz, F.; Ahmad, Z.; Rafique, S.; Wageh, S.; Al-Ghamdi, A. A.; Sulaiman, K.; Touati, F.; Shakoor, R. A.; Al-Thani, N. J., Structural, morphological and optical properties of PEDOT:PSS/QDs nano-composite films prepared by spin-casting. *Physica E: Low Dimens. Syst. Nanostruct.* **2016**, *83*, 64-68, DOI: <http://dx.doi.org/10.1016/j.physe.2016.04.014>.
- [22] Rebiś, T.; Milczarek, G., A comparative study on the preparation of redox active bioorganic thin films based on lignosulfonate and conducting polymers. *Electrochim. Acta* **2016**, *204*, 108-117, DOI: <http://dx.doi.org/10.1016/j.electacta.2016.04.061>.
- [23] Fu, Y.; Cheng, H.; Elsenbaumer, R. L., Electron-rich thienylene-vinylene low bandgap polymers. *Chem. Mater.* **1997**, *9*, 1720-1724, DOI: 10.1021/cm960399j.
- [24] Huang, H.; Pickup, P. G., A Donor-acceptor conducting copolymer with a very low band gap and high intrinsic conductivity. *Chem. Mater.* **1998**, *10*, 2212-2216, DOI: 10.1021/cm9801439.
- [25] Alemán, C.; Casanovas, J., Theoretical investigation of the 3,4-ethylenedioxythiophene dimer and unsubstituted heterocyclic derivatives. *J. Phys. Chem. A* **2004**, *108*, 1440-1447, DOI: 10.1021/jp0369600.
- [26] Shi, W.; Zhao, T.; Xi, J.; Wang, D.; Shuai, Z., Unravelling doping effects on PEDOT at the molecular level: From geometry to thermoelectric transport properties. *J. Am. Chem. Soc.* **2015**, *137*, 12929-12938, DOI: 10.1021/jacs.5b06584.
- [27] Zhang, B.; Wang, K.; Li, D.; Cui, X., Doping effects on the thermoelectric properties of pristine poly(3,4-ethylenedioxythiophene). *RSC Advances* **2015**, *5*, 33885-33891, DOI: 10.1039/C4RA16451B.
- [28] Dkhissi, A.; Louwet, F.; Groenendaal, L.; Beljonne, D.; Lazzaroni, R.; Brédas, J. L., Theoretical investigation of the nature of the ground state in the low-bandgap conjugated polymer, poly(3,4-ethylenedioxythiophene). *Chem. Phys. Lett.* **2002**, *359*, 466-472, DOI: [http://dx.doi.org/10.1016/S0009-2614\(02\)00651-6](http://dx.doi.org/10.1016/S0009-2614(02)00651-6).
- [29] Agbaoye, R. O.; Adebambo, P. O.; Akinlami, J. O.; Afolabi, T. A.; Karazhanov, S. Z.; Ceresoli, D.; Adebayo, G. A., Elastic constants and mechanical properties of PEDOT from first principles calculations. *Comput. Mater. Sci.* **2017**, *139*, 234-242, DOI: <http://dx.doi.org/10.1016/j.commatsci.2017.07.042>.
- [30] Zhou, J.; Anjum, D. H.; Chen, L.; Xu, X.; Ventura, I. A.; Jiang, L.; Lubineau, G., The temperature-dependent microstructure of PEDOT/PSS films: insights from morphological, mechanical and electrical analyses. *J. Mater. Chem. C* **2014**, *2*, 9903-9910, DOI: 10.1039/C4TC01593B.

- [31] Wang, F.; Wilson, M. S.; Rauh, R. D.; Schottland, P.; Thompson, B. C.; Reynolds, J. R., Electrochromic linear and star branched poly(3,4-ethylenedioxythiophene-didodecyloxybenzene) polymers. *Macromolecules* **2000**, *33*, 2083-2091, DOI: 10.1021/ma9918506.
- [32] Heuer, H. W.; Wehrmann, R.; Kirchmeyer, S., Electrochromic window based on conducting poly(3,4-ethylenedioxythiophene)-poly(styrene sulfonate). *Adv. Function. Mater.* **2002**, *12*, 89-94, DOI: 10.1002/1616-3028(20020201)12:2<89::AID-ADFM89>3.0.CO;2-1.
- [33] Dyer, A. L.; Thompson, E. J.; Reynolds, J. R., Completing the color palette with spray-processable polymer electrochromics. *ACS Appl. Mater. Interfaces* **2011**, *3*, 1787-1795, DOI: 10.1021/am200040p.
- [34] Colak, B.; Büyükkoyuncu, A.; Baycan Koyuncu, F.; Koyuncu, S., Electrochromic properties of phenantrene centered EDOT polymers. *Polymer* **2017**, *123*, 366-375, DOI: <http://dx.doi.org/10.1016/j.polymer.2017.07.035>.
- [35] Lin, T. -H.; Ho, K. -C., A complementary electrochromic device based on polyaniline and poly(3,4-ethylenedioxythiophene). *Solar Energy Mater. Solar Cells* **2006**, *90*, 506-520, DOI: <http://dx.doi.org/10.1016/j.solmat.2005.02.017>.
- [36] El-Enany, G. M.; Ghanem, M. A.; El-Ghaffar, M. A. A., Electrochemical deposition and characterization of poly(3,4-ethylene dioxythiophene), poly(aniline) and their copolymer onto glassy carbon electrodes for potential use in ascorbic acid oxidation. *Portugaliae Electrochimica Acta* **2010**, *28*, 336-348, [http://www.scielo.mec.pt/scielo.php?script=sci\\_arttext&pid=S0872-19042010000500005&nrm=iso](http://www.scielo.mec.pt/scielo.php?script=sci_arttext&pid=S0872-19042010000500005&nrm=iso).
- [37] Ohlan, A.; Singh, K.; Chandra, A.; Dhawan, S. K., Conducting ferromagnetic copolymer of aniline and 3,4-ethylenedioxythiophene containing nanocrystalline barium ferrite particles. *J. Appl. Polym. Sci.* **2008**, *108*, 2218-2225, DOI: 10.1002/app.27794.
- [38] Shahhosseini, L.; Nateghi, M. R.; Kazempour, M.; Borhani Zarandi, M., Electrochemical synthesis of novel polymer based on (4-(2,3-dihydrothieno[3,4-6][1,4][dioxin-5-yl) aniline) in aqueous solution: Characterization and application. *Mater. Chem. Phys* **2016**, *177*, 554-563, DOI: <http://dx.doi.org/10.1016/j.matchemphys.2016.04.069>.
- [39] Frisch, M. J.; Trucks, G. W.; Schlegel, H. B.; Scuseria, G. E.; Robb, M. A.; Cheeseman, J. R.; Scalmani, G.; Barone, V.; Mennucci, B.; Petersson, G. A.; Nakatsuji, H.; Caricato, M.; Li, X.; Hratchian, H. P.; Izmaylov, A. F.; Bloino, J.; Zheng, G.; Sonnenberg, J. L.; Hada, M.; Ehara, M.; Toyota, K.; Fukuda, R.; Hasegawa, J.; Ishida, M.; Nakajima, T.; Honda, Y.; Kitao, O.; Nakai, H.; Vreven, T.; Montgomery Jr., J. A.; Peralta, J. E.; Ogliaro, F.; Bearpark, M. J.; Heyd, J.; Brothers, E. N.; Kudin, K. N.; Staroverov, V. N.; Kobayashi, R.; Normand, J.; Raghavachari, K.; Rendell, A. P.; Burant, J. C.; Iyengar, S. S.; Tomasi, J.; Cossi, M.; Rega, N.; Millam, N. J.; Klene, M.; Knox, J. E.; Cross, J. B.; Bakken, V.; Adamo, C.; Jaramillo, J.; Gomperts, R.; Stratmann, R. E.; Yazyev, O.; Austin, A. J.; Cammi, R.; Pomelli, C.; Ochterski, J. W.; Martin, R. L.; Morokuma, K.; Zakrzewski, V. G.; Voth, G. A.; Salvador, P.; Dannenberg, J. J.; Dapprich, S.; Daniels, A. D.; Farkas, Ö.; Foresman, J. B.; Ortiz, J. V.; Cioslowski, J.; Fox, D. J. Gaussian 09, Gaussian, Inc.: Wallingford, CT, USA, 2009.
- [40] Pandey, L.; Risko, C.; Norton, J. E.; Brédas, J. -L., Donor-acceptor copolymers of relevance for organic photovoltaics: A theoretical investigation of the impact of chemical structure modifications on the electronic and optical properties. *Macromolecules* **2012**, *45*, 6405-6414, DOI: 10.1021/ma301164e.
- [41] Zhang, L.; Pei, K.; Yu, M.; Huang, Y.; Zhao, H.; Zeng, M.; Wang, Y.; Gao, J., Theoretical investigations on donor-acceptor conjugated copolymers based on naphtho[1,2-c:5,6-c']bis[1,2,5]thiadiazole for organic solar cell applications. *J. Phys. Chem. C* **2012**, *116*, 26154-26161, DOI: 10.1021/jp306656c.
- [42] Sahu, H.; Panda, A. N., Computational study on the effect of substituents on the structural and electronic properties of thiophene-pyrrole-based  $\pi$ -conjugated oligomers. *Macromolecules* **2013**, *46*, 844-855, DOI: 10.1021/ma3024409.

- [43] Franco, F. C.; Padama, A. A. B., DFT and TD-DFT study on the structural and optoelectronic characteristics of chemically modified donor-acceptor conjugated oligomers for organic polymer solar cells. *Polymer* **2016**, *97*, 55-62, DOI: <https://doi.org/10.1016/j.polymer.2016.05.025>.
- [44] Garcia, M.; Fomina, L.; Fomine, S., Electronic structure evolution of neutral and dicationic states of conjugated polymers with their band gap. *Synthetic Metals* **2010**, *160*, 2515-2519, DOI: <http://dx.doi.org/10.1016/j.synthmet.2010.09.037>.
- [45] Chiang, C. K.; Fincher, C. R.; Park, Y. W.; Heeger, A. J.; Shirakawa, H.; Louis, E. J.; Gau, S. C.; MacDiarmid, A. G., Electrical conductivity in doped polyacetylene. *Physical Review Letters* **1977**, *39*, 1098-1101, <http://link.aps.org/doi/10.1103/PhysRevLett.39.1098>.
- [46] Kamran, M.; Ullah, H.; Shah, A.-u.-H. A.; Bilal, S.; Tahir, A. A.; Ayub, K., Combined experimental and theoretical study of poly(aniline-co-pyrrole) oligomer. *Polymer* **2015**, *72*, 30-39, DOI: <http://dx.doi.org/10.1016/j.polymer.2015.07.003>.
- [47] Shahhosseini, L.; Nateghi, M. R.; Kazempour, M.; Zarandi, M. B., Electrochemical synthesis of polymer based on 4-(2-furyl) benzenamine: Electrochemical properties, characterization and applications. *Progress in Org. Coatings* **2015**, *88*, 272-282, DOI: <http://dx.doi.org/10.1016/j.porgcoat.2015.07.014>.
- [48] Shahhosseini, L.; Nateghi, M. R.; SheikhSivandi, S., Electrochemical synthesis of polymer based on 4-(2-thienyl)benzenamine in aqueous solutions: Electrochemical properties, characterization and application. *Synthetic Metals* **2016**, *211*, 66-74, DOI: <http://dx.doi.org/10.1016/j.synthmet.2015.11.015>.
- [49] Franco Jr, F. C.; Padama, A. A. B., DFT and TD-DFT study on the structural and optoelectronic characteristics of chemically modified donor-acceptor conjugated oligomers for organic polymer solar cells. *Polymer* **2016**, *97*, 55-62, DOI: <http://dx.doi.org/10.1016/j.polymer.2016.05.025>.
- [50] Rosmus, P.; Bock, H.; Solouki, B.; Maier, G.; Mihm, G., Silaethene: Highly correlated wave functions and photoelectron spectroscopic evidence. *Angewandte Chemie Int. Ed. in English* **1981**, *20*, 598-599, DOI: 10.1002/anie.198105981.